

Simulation of Tsunami impact upon Coastline

Aristotelis Spathis-Papadiotis¹ and Konstantinos Moustakas¹

Electrical and Computer Engineering Department
University of Patras, Patra, Greece
moustakas@upatras.gr

Abstract. This paper presents a simulation of a tsunami impact upon an urban coastline. Emphasis was given to the conservation of momentum, as its distribution in space and time is the main factor of the wave's effects on the coastline. Due to this, a hybrid simulation method was adopted, based on the Smoothed Particle Hydrodynamics (SPH) method, enriched with geometric constraints and rigid body interactions. The implementation is the result of cooperation between the Bullet physics engine and our custom SPH engine, which successively process the dynamic state of the fluid at every timestep. Furthermore, in order to achieve better performance a custom data structure (LP grid) was developed for the optimization of locality in data storage and minimization of access time. Simulation data is exported to VTK files, allowing interactive processing and visualization. Experimental results demonstrate the benefits of impulse recording at potential hazard estimation and evaluation of defense strategies.

Keywords: Fluid simulation, tsunami, SPH, tsunami-coastline interaction, force visualization

1 Introduction

Simulations of natural phenomena are a precious tool for analysis and understanding of the processes behind them as well as the implications of those. Especially fluid dynamics is one of the fields most benefitted by the explosive growth of high performance parallel computing architectures of the last years. Tsunamis are one of the most devastating natural disasters, with much attention drawn to them lately, especially after the 2004 Indian Ocean tsunami and the 2011 Tōhoku earthquake and tsunami, two of the largest incidents in modern history. Multiscale modelling of tsunami generation, propagation and impact is a trending research area as respective simulations give valuable insights into the underlying mechanisms and relations between the various stages of an unfolding tsunami incident, while also facilitating the assessment of potential hazard it poses upon impact on a coastline.

A tsunami is a series of waves in a water body caused by an impulsive disturbance that vertically displaces a large volume of water. Tsunamis are generated by earthquakes, volcanic eruptions, landslides and other such events which have

the potential to transmit a huge amount of mechanical energy to an overlying or adjacent water volume. On a macroscopic level, tsunami propagation across the ocean as well as coastline inundation and runup are usually simulated through methods based on various versions of the shallow water equations, which are derived from the Navier-Stokes equations if the horizontal length scale is much greater than the vertical one. Conversely, the aforementioned methods are not appropriate in smaller scale simulations of the impact upon the coastline, since in order to obtain a reliable estimation of the forces exerted on the terrain, complex dynamics of fluid-structure interactions have to be accounted for. One of the most used methods for simulating complex flows with multiple boundary interactions is Smoothed Particle Hydrodynamics, initially proposed in the 1970s for the treatment of compressible flows in astrophysical problems. The method has enjoyed extensive adoption, having been applied to numerous fields ranging from aerodynamics and geology to engineering and computer graphics with exceptional results, lending itself well to adaptations and extensions. The main contribution of our approach is the emphasis given to the explicit conservation of momentum and the detailed data collection and visualization relating to its distribution upon the coastline during the tsunami impact. Towards this end, we adopted SPH enriched with geometric constraints as our method of choice due to the unparalleled advantages it offers, directly linked to its properties as a lagrangian method.

2 Related Work

Computational fluid dynamics is a very active area of research, as it relates to a wide spectrum of applications in computer graphics, engineering and science. The SPH method was developed independently by Gingold and Monaghan [8] and Lucy [14] in 1977. Since then, it has been employed in a wide variety of problems and applications, proving itself to be a flexible and attractive method for the simulation of complex, multicomponent/multiphase flows. Its flexibility is shown by the numerous adaptations and customizations it has undergone to suit many diverse problem domains.

Tsunami simulations have been shown to be a valuable tool in the literature, aiding in estimation of key parameters of a tsunami incident, such as its propagation course and coastal inundation. Simulations of the devastating 2004 Indian Ocean tsunami have been carried out by Wang and Liu [20] and Ioualalen et al. [11], using nonlinear shallow water equations and nonlinear Boussinesq models respectively. In both cases, good agreement between calculations and field measurements of inundation and runup indicate the robustness of these approaches. Samaras et al. [17] used a 2D horizontal model based on the higher oder Boussinesq equations to simulate tsunami-induced coastal inundation in two relevant areas of interest in the Mediterranean. Using two different models, Kakinuma [12] reproduced a past incident with sufficient accuracy. The governing equations for both were the continuity and Reynolds equations for incompressible fluids in

porous media, while water surface displacement was determined by the vertically integrated continuity equation for the first and the 3D Volume of Fluid method for the second model.

Relating to the SPH method, Desbrun and Gascuel [6] used it to animate highly deformable bodies of various stiffness and viscosity, while proposing important extensions like the “spiky” pressure smoothing kernel and discussing implementation issues such as the fluid surface reconstruction from density isosurfaces. Later, Müller et al. [16] used this work as a basis for fluid simulation in interactive applications. Becker and Teschner [2] developed Weakly Compressible SPH, where the ideal gas equation of state is replaced with the much more strict Tait equation to reduce compressibility to a user-defined upper bound, thus avoiding an inefficient explicit Poisson equation solver. In recent years, Solenthaler and Pajarola [18] improved WCSPH by proposing Predictive-Corrective Incompressible SPH, where a prediction-correction scheme is used to compute particle pressures through iterative density constraint satisfaction and propagation through the fluid, until the final tolerance conditions are met. Implicit Incompressible SPH was then proposed by Ihmsen et al. [10], in which the density is predicted using a discretized form of the pressure Poisson equation, as obtained from the combination of a direct discretization of the continuity equation and symmetric pressure forces.

SPH has been employed in many simulations involving wave-coastline interactions. Debroux et al. [5] used SPH for the simulation of tsunami impact on real coastline topography, where important features like the energy and speed of the wave were measured over the course of time. Gómez-Gesteira and Dalrymple [9] simulated the impact of a wave generated by a dam break against a tall structure with a 3D SPH method, showing good agreement with lab measurements of velocities and forces. Dalrymple and Rogers [3] gave a comprehensive overview of techniques regarding usage of SPH for simulation of water waves and their interaction with structures, while also highlighting its suitability for close-up examinations of small regions. Many studies have considerably improved upon this line of research, yielding exceptional results. For example, St-Germain et al. [19] used a 3D WCSPH model to examine and analyze spatially and temporally forces exerted by tsunami-like hydraulic bore upon freestanding structures.

Due to its generality and adaptability, SPH has been the method of choice for many applications and relative extensions. Macklin and Müller [15] enriched SPH with positional geometric constraints, thus enforcing incompressibility while maintaining stability and allowing for large timesteps. Rigid-fluid interaction is one of the strong aspects of the method, as is shown by Akinci et al. [1], where rigid surfaces are sampled by boundary particles, which adaptively contribute to fluid properties to address boundary region deficiencies and inhomogeneities, in order to incorporate rigid bodies to a unified hydrodynamic framework. Finally, a thorough overview of various implementation algorithms and data structures

together with their advantages and drawbacks is provided by Domínguez et al. [7].

3 Proposed framework

Our proposed simulation framework is based on SPH, a lagrangian fluid simulation method whose core notion is the discretization of the fluid into particles, which serve as interpolation points for the estimation of fluid properties in space. Advantages of this method include the exact treatment of advection, the natural way of dealing with special interface interactions, the inherent conservation of significant quantities (mass, momentum, energy) and the self-adaptivity of computational load to the fluid location and state in the flow domain. To efficiently ensure incompressibility in degenerate cases and undersampled boundary regions while maintaining relatively large timesteps, SPH was enhanced with explicit solving of geometric constraints between particles. These constraints are solved by the Bullet physics engine, within which fluid particles are represented as rigid bodies, while also being subject to SPH forces as computed at each timestep of the simulation.

3.1 SPH method

Starting from the identity:

$$f(\mathbf{r}) = \int_V f(\mathbf{x})\delta(\mathbf{r} - \mathbf{x})d\mathbf{x},$$

where $\delta(\mathbf{r})$ the Dirac delta function and $\mathbf{x} \in V$, one can obtain a more general interpolation rule by substituting $\delta(\mathbf{r})$ with a smoothing kernel $W(\mathbf{r}, h)$:

$$f(\mathbf{r}) \approx \int_V f(\mathbf{x})W(\mathbf{r} - \mathbf{x}, h)d\mathbf{x}$$

whose limit when $h \rightarrow 0$ approaches the delta function and is normalized to unity:

$$\lim_{h \rightarrow 0} W(\mathbf{r}, h) = \delta(\mathbf{r}) \quad \text{and} \quad \int_V W(\mathbf{r}, h)d\mathbf{x} = 1$$

The smoothing radius h serves as a cutoff radius in the smoothing process, as particles beyond that distance have no contribution to the sum, i.e. $W(r, h) = 0$ when $r > h$. For the discrete case, where f is discretized to particles with density ρ and mass m , the weighting ratio m/ρ can be used to construct a weighted sum interpolant for any field A :

$$A(\mathbf{r}) = \sum_i \frac{m_i}{\rho_i} A(\mathbf{r}_i) W(\mathbf{r} - \mathbf{r}_i, h) \quad (1)$$

which lies at the heart of SPH formulation. According to this, the gradient can be computed by the following approximation:

$$\nabla A(\mathbf{r}) = \sum_i \frac{m_i}{\rho_i} A(\mathbf{r}_i) \nabla W(\mathbf{r} - \mathbf{r}_i, h) \quad (2)$$

The obvious advantage of this is the exclusive dependence on the smoothing kernel gradient, which can be precomputed for sensible kernel choices. However, this formula can lead to unsymmetric pair forces, compromising the conservation of linear and angular momentum of the system. To symmetrize these forces depending on gradients (like those originating from pressure differences), we can use the product rule:

$$\nabla \left(\frac{P}{\rho} \right) = \frac{\nabla P}{\rho} - \frac{P}{\rho^2} \nabla \rho \quad \Leftrightarrow \quad \nabla P = \rho \left[\frac{P}{\rho^2} \nabla \rho + \nabla \left(\frac{P}{\rho} \right) \right]$$

to obtain an alternative approximation of gradient

$$\begin{aligned} \nabla P &= \rho \left[\frac{P}{\rho^2} \sum_i \frac{m_i}{\rho_i} \rho_i \nabla W(\mathbf{r} - \mathbf{r}_i, h) + \sum_i \frac{m_i}{\rho_i} \frac{P_i}{\rho_i} \nabla W(\mathbf{r} - \mathbf{r}_i, h) \right] \\ &= \rho \sum_i m_i \left(\frac{P}{\rho^2} + \frac{P_i}{\rho_i^2} \right) \nabla W(\mathbf{r} - \mathbf{r}_i, h) \end{aligned} \quad (3)$$

which is antisymmetric for all interacting particle pairs. Viscosity forces on the other hand, are proportional to the laplacian of the velocity field:

$$\nabla^2 \mathbf{v} = \sum_i \frac{m_i}{\rho_i} (\mathbf{v}_i - \mathbf{v}) \nabla^2 W(\mathbf{r} - \mathbf{r}_i, h) \quad (4)$$

and are always antisymmetric, since they depend on velocity difference $\mathbf{v}_i - \mathbf{v}$ between particles. In each timestep of the simulation, the density of all particles is first computed according to equation (2), as it depends only on the relative position of those. The pressure at each particle location is then obtained from its respective density through an equation of state. After this step, the pressure and viscosity forces are computed from the particle data and integrated back into the position and velocity of the particles.

3.2 Implementation

Simulation initialization Each simulation under our implementation consists of two elements, the coastline terrain (static) and the tsunami wave (dynamic). For the simulation setup, terrain is imported from a suitable 3D geometry definition file format, the initial conditions of the impacting wave (position and velocity) are configured and the desired discretization resolution for the fluid (i.e. the number of particles it is discretized into) is set. From these conditions, the terrain and fluid are initialized and key parameters are computed as subsequently described. Terrain geometry is uniformly scaled by a user-supplied

factor and docked to the origin of coordinates and the particle effective radius r is determined such that the specified discretization resolution is achieved. Fluid particles are initially placed on a Hexagonal Close-Packed lattice covering the fluid initial position, in order to accomplish the densest possible packing and symmetry:

$$[x, y, z] = \left[2i + [(j+k) \bmod 2], \sqrt{3}[j + \frac{1}{3}(k \bmod 2)], \frac{2\sqrt{6}}{3}k \right] r \quad (5)$$

In this configuration, the smoothing radius h is computed such that each particle has approximately 50 neighbours (following the empirical rule established in the literature). The timestep is calculated according to the Courant-Friedrichs-Lowy criterion:

$$\delta t_{\text{CFL}} = C \frac{\delta x}{v_{\max}}, \quad (6)$$

for values of Courant number $C \approx 0.5$ with characteristic length δx equal to the particle effective radius and maximum velocity v_{\max} determined by the maximum potential energy in the initial configuration.

SPH parameters Following standard practice, we used three different smoothing kernels for density, pressure gradient and velocity laplacian computation, respectively:

$$W_{\text{poly6}}(r, h) = \frac{315}{64\pi h^9} \begin{cases} (h^2 - r^2)^3 & 0 \leq r \leq h \\ 0 & \text{otherwise} \end{cases} \quad (7)$$

$$W_{\text{spiky}}(r, h) = \frac{15}{\pi h^6} \begin{cases} (h - r)^3 & 0 \leq r \leq h \\ 0 & \text{otherwise} \end{cases} \quad (8)$$

$$\nabla W_{\text{spiky}}(r, h) = \frac{-45}{\pi h^6} (h - r)^2$$

$$W_{\text{viscosity}}(r, h) = \frac{15}{2\pi h^3} \begin{cases} -\frac{r^3}{2h^3} + \frac{r^2}{h^2} + \frac{h}{2r} - 1 & 0 \leq r \leq h \\ 0 & \text{otherwise}, \end{cases} \quad (9)$$

$$\nabla^2 W_{\text{viscosity}}(r, h) = \frac{45}{\pi h^6} (h - r)$$

In each simulation step iteration, W_{poly6} is used as smoothing kernel for the fluid density estimation at each particle, based on its neighbour particle locations. W_{spiky} and $W_{\text{viscosity}}$ are substituted into equations (3) and (4), in order to compute forces arising from pressure differences and viscosity, respectively. Fluid pressure is obtained from the estimated fluid density through the ideal gas equation of state:

$$P = k(\rho - \rho_0), \quad (10)$$

according to which the pressure is proportional to the difference of the current from the rest density. The major problem with this equation of state are the

compressibility issues that have been shown to exist in simulations using it. A frequently proposed solution is to replace the above with the Tait equation of state:

$$P = B \left(\left(\frac{\rho}{\rho_0} \right)^\gamma - 1 \right), \quad (11)$$

where usually $\gamma = 7$ and B is a proportionality constant controlling the tolerance for density fluctuations. This equation is much more punishing on density fluctuations away from the rest density, therefore requiring significantly smaller timesteps to ensure stability.

Enhancements to SPH In our framework we opted for a different solution, inspired by Position Based Fluids [15], in which particles are represented by spherical rigid bodies. The most important advantage of this technique is the elegant handling of boundary, undersampled and degenerate fluid regions that tend to arise very frequently in simulations of free flows. The adoption of this approach allows to treat boundary collisions in a simple manner, while naturally enforcing incompressibility near boundaries and free surfaces. In these regions, estimators fail to describe the actual flow regime due to neighbour particle shortage. This undersampling creates the need for correction procedures, usually involving ghost/boundary particles, to avoid pressure instabilities, particle clustering and other artifacts. On the contrary, no such method is necessary under our representation, where degenerative cases are handled through geometric constraints, thus selectively preventing unreliable estimations from affecting the flow.

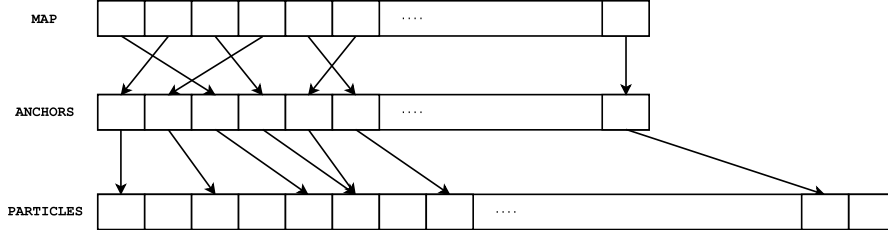


Fig. 1. Organization of the custom data structure designed for the efficient storing and interaction scanning between simulation particles. Top-down, the first vector implements the 3D to linear locality preserving mapping of cell anchors onto the second, which in turn points to each cell's particles on the third.

Data organization and export Rigid body dynamics are handled by the Bullet physics engine. A custom cell list data structure (LP grid) was implemented in order to optimize particle dynamic storage and access time. The simulation

domain is divided by a regular 3D grid of spacing equal to the smoothing radius into cubic cells containing the fluid particles. Particles are generated as Bullet objects and are stored in the LP grid, which consists of three storage vectors. As shown in Figure 1, particles are accessed by following pointers through those vectors in order. The `map` vector contains pointers to `anchors` and in turn `anchors` pointers to `particles`, which contains the simulation particles. Each cell's particles are continuously stored in the `particles` vector. Each element of `anchors` represents a cell and contains a pointer to the start of the region that contains that cell's particles in `particles`. Since SPH access patterns are heavily reliant on neighbour searching, increasing the locality in the linear order in which cells are stored is clearly beneficial to performance, due to better utilization of cache memory. For that reason, cells are represented spatially sorted along a space-filling curve in `anchors` (and consequently, `particles`), in order to maximize locality preservation from the 3D simulation domain to the linear storage. To efficiently address the cells, one extra layer encoding the locality preserving mapping has to be added, in the form of the first vector `map`. To access a cell, the three indices i_x, i_y, i_z specifying its position in the grid are converted to a linear index i (a simple way is through the formula $i = i_z * N_y * N_x + i_y * N_x + i_x$, where N_x, N_y, N_z is the number of cells along the x, y and z axis in the grid respectively). The `map` vector serves as a lookup table, so that its i -th element contains the pointer to that cell's representation on `anchors`. LP grid advantages include cohesive storage, quick neighbour search and interaction scanning, exploitation of the SPH algorithm access patterns and fast, in-place update.

Simulation is following the Bullet framework, with the SPH code being embedded as an internal timestep tick callback function. We took advantage of the Bullet infrastructure to extract detailed information about the collisions between fluid and terrain regarding the resulting impulse, time and location. Impulse and particle data are then written to multiple VTK files per frame. Samples of the smoothed color field (common name in the literature for the field having the value 1 at particle locations and 0 everywhere else) on the regular cell lattice are also exported, which are then used to reconstruct the fluid surface as an isosurface of that field. At the end of the simulation a cumulative impulse heatmap along with the scaled and docked terrain model is also provided.

4 Results

Multiple simulations were carried out using different models of urban coastline, in order to gain a significant and diverse dataset of impulses exerted over the duration of the impact. Tsunamis are vastly different from the usual wind-induced sea waves in that they have far longer wavelength and carry much greater total energy, appearing as a rapidly rising tide instead of breaking waves. Accounting for these facts, we chose to represent the tsunami wave as a water volume invading the coastline with an initial velocity.

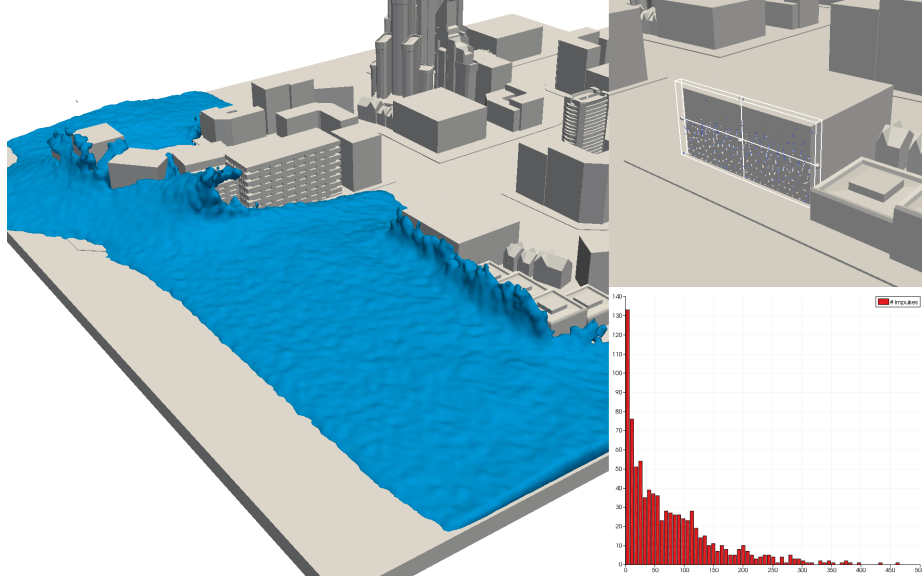


Fig. 2. Example visualization of impact data in ParaviewTM. Fluid surface is reconstructed as an isosurface of the color field, while impulses on the selected region are visualized as points on the 3D terrain model and in a histogram grouped by their magnitude.

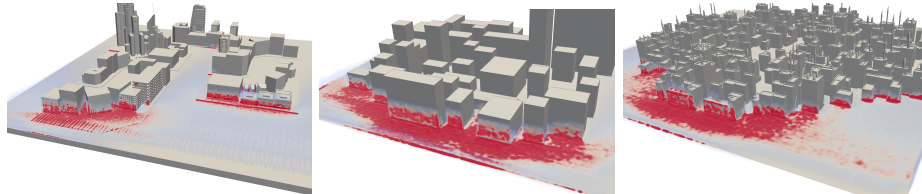


Fig. 3. Tsunami impulse heatmaps for three different urban models visualized under ParaviewTM. Most of the energy of the waves is absorbed by the first obstacle in their way.

Figure 2 shows a typical simulation result with the aid of ParaviewTM, where the reconstructed wave surface and impulses exerted on a selected region are visualized along the 3D terrain model and plotted on a histogram. Figure 3 shows impulse heatmaps generated by simulation of tsunami impact upon three different urban terrain models. The base ground width and depth of the models are in the order of 100 metres and the fluid is discretized into 80k particles, having an initial velocity of 10m/s. Simulation time for each model was about 40 minutes on a x86_64 GNU/Linux desktop computer with an IntelTM i7-3770 processor and 8GB of main memory, accounting for 5 seconds of simulated time.

A comparison of the resulting impulse heatmap from the same tsunami impact upon an exposed coastline and one with a protective seawall is shown in Figure 4. These heatmaps confirm a well-documented observation in the literature, i.e. that tsunami energy is absorbed mostly by the first obstacle in its way. This has been noted by Danielsen et al. [4] and Kathiresan and Narayanasamy [13], who both emphasized the protective role coastal vegetation (mangrove forests) played in mitigating the impact effects of the 2004 Indian Ocean tsunami. The same conclusion has been reached by Yanagisawa et al. [21] through theoretical approximation of the phenomenon backed by relevant field data and measurements. Seawalls have been constructed in high-risk regions as a common countermeasure against tsunami hazards. Although the waves may be so large as to overtop such barriers, these cases are somewhat rare, making seawalls an effective first line of defense.

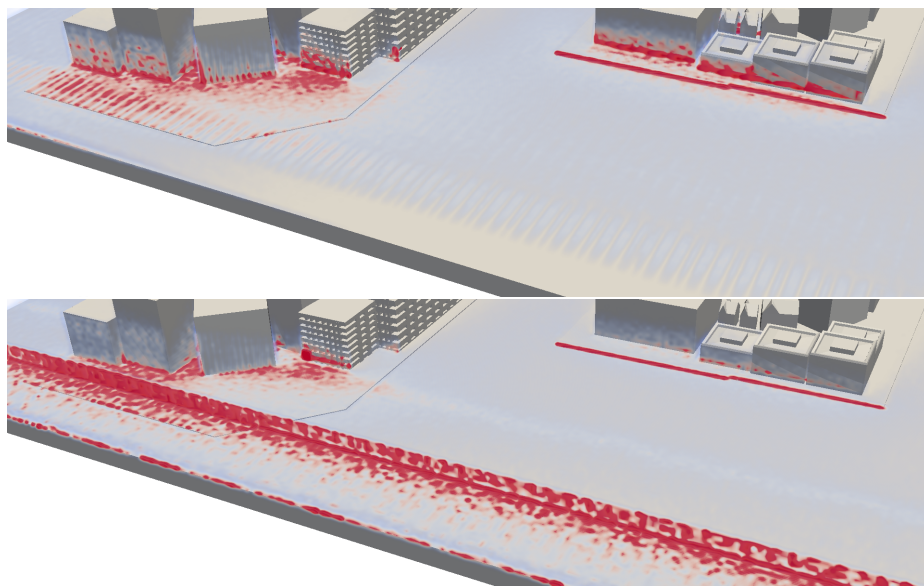


Fig. 4. Comparison between the impulse heatmap of a tsunami hit on the same urban coastline model, with (up) and without (down) the protection from a seawall. Seawalls are commonly found in high-risk areas, as they reduce impact effects significantly.

The performance of the simulation program was satisfactory, there is however a substantial margin for improvement. Figure 5 shows a plot of the mean computation time per internal timestep for variable fluid resolution. It is important to note that a higher number of simulation particles imposes a shorter internal timestep due to their smaller effective radius. These measurements are also representative of the worst-case scenario, as due to the initial fluid conditions the

particles are closely packed in a single body of fluid, thus having maximum number of mutual interactions and reducing the performance gains from our spatial hashing data structure. About 75% of runtime is spent in single-threaded code consisting mostly of Bullet and I/O operations, while the rest corresponds to multi-threaded code of our SPH engine.

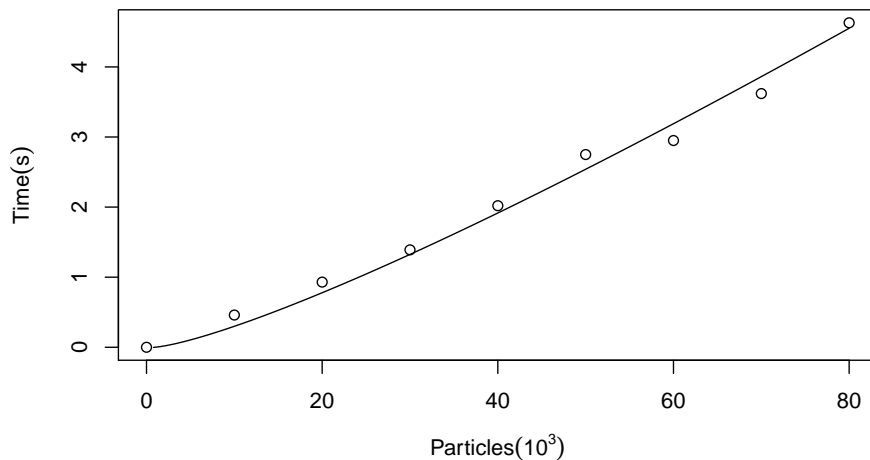


Fig. 5. Plot showing the mean simulation time (in seconds) per internal timestep for the first 10 output frames (each frame was set to 0.05 seconds of simulated time), for 10k to 80k particles (continuous line represents $O(n \log_2 n)$ growth).

Although our framework provides rich and detailed data, a quantitative comparison to either field measurements or results of other methods utilizing different versions of the SPH formulations couldn't be reliably made. We haven't yet implemented a way to configure the wave's initial conditions and coastline terrain to model the impact according to predictions of large scale simulations or data from past incidents. Qualitatively, our method seems to compare well to similar codes utilizing SPH to simulate small scale tsunami interactions with coastline structures. Other methods usually make use of SPH enhancements originating from the CFD literature, which aim to improve some aspect of the flow (for example incompressibility, regarding WCSPH). In this particular application domain though, boundary interactions can be arguably considered more important than the flow itself. Our approach, enriching SPH with direct positional constraint solving, shows promise as an efficient way for dealing explicitly and exactly with momentum preservation and detailed fluid-structure impulse recording.

5 Conclusions

We presented the theoretical background and implementation of an enriched SPH framework, whose main purpose was the faithful simulation and detailed recording of the forces exerted upon the coastline during a tsunami impact. The chosen output file format lends itself to rich visualizations, allowing for a quick overview of complex simulation data. Multiple simulations have been carried out, resulting in interesting visualizations of impact data and evaluation of defense mechanisms. Furthermore, detailed impulse logs are provided, which can then be processed to extract relevant high level information. Possible future extensions could be the incorporation of wider, dynamic terrain models, including nearby seabed, the adjustment of the fluid initial conditions to match those predicted by large scale shallow water or Boussinesq models and performance optimizations in the implementation towards a more integrated dataflow scheme.

References

1. Akinci, N., Ihmsen, M., Akinci, G., Solenthaler, B., Teschner, M.: Versatile rigid-fluid coupling for incompressible SPH. *ACM Transactions on Graphics (TOG)* 31(4), 62:1–62:8 (2012)
2. Becker, M., Teschner, M.: Weakly compressible SPH for free surface flows. In *Proceedings of the 2007 ACM SIGGRAPH/Eurographics symposium on Computer animation*, 209–217 (2007)
3. Dalrymple, R. A., Rogers, B. D.: Numerical modeling of water waves with the SPH method. *Coastal engineering* 53(2), 141–147 (2006)
4. Nielsen, F., Sørensen, M. K., Olwig, M. F., Selvam, V., Parish, F., Burgess, N. D., Hiraishi, T., Karunagaran, V. M., Rasmussen, M. S., Hansen, L. B. and Quarto, A.: The Asian tsunami: a protective role for coastal vegetation. *Science(Washington)* 310(5748), 643 (2005)
5. Debroux, F., Prakash, M., Cleary, P.: Three-dimensional modelling of a tsunami interacting with real topographical coastline using Smoothed Particle Hydrodynamics. *Proceedings of the 14th Australasian Fluid Mechanics Conference, Adelaide, Australia*, 311–314 (2001)
6. Desbrun M., Cani, M. P.: Smoothed particles: A new paradigm for animating highly deformable bodies. In *Computer Animation and Simulation 96 (Proceedings of EG Workshop on Animation and Simulation)*, 61–76 (1996)
7. Domínguez, J. M., Crespo, A. J., Gómez-Gesteira, M., Marongiu, J. C.: Neighbour lists in smoothed particle hydrodynamics. *International Journal for Numerical Methods in Fluids* 67(12), 2026–2042 (2011)
8. Gingold, R. A., Monaghan, J. J.: Smoothed particle hydrodynamics: theory and application to non-spherical stars. *Monthly notices of the royal astronomical society* 181(3), 375–389 (1977)
9. Gómez-Gesteira, M., Dalrymple, R. A.: Using a three-dimensional smoothed particle hydrodynamics method for wave impact on a tall structure. *Journal of Waterway, Port, Coastal and Ocean Engineering* 130(2), 63–69 (2004)
10. Ihmsen, M., Cornelis, J., Solenthaler, B., Horvath, C., Teschner, M.: Implicit incompressible SPH. *Visualization and Computer Graphics, IEEE Transactions on* 20(3), 426–435 (2014)

11. Ioualalen, M., Asavanant, J., Kaewbanjak, N., Grilli, S. T., Kirby, J. T., Watts, P.: Modeling the 26 December 2004 Indian Ocean tsunami: Case study of impact in Thailand. *Journal of Geophysical Research: Oceans* 112(C7), (2007)
12. Kakinuma, T.: 3D numerical simulation of tsunami runup onto a complex beach. *Advanced numerical models for simulating tsunami waves and runup*, 255–260 (2008)
13. Kathiresan, K., Rajendran, N.: Coastal mangrove forests mitigated tsunami. *Estuarine, Coastal and Shelf Science* 65(3), 601–606 (2005)
14. Lucy, L. B.: A numerical approach to the testing of the fission hypothesis. *The astronomical journal* 82, 1013–1024 (1977)
15. Macklin, M., Müller, M.: Position Based Fluids. *ACM Trans. Graph.* 32(4), 104:1–104:12 (2013)
16. Müller, M., Charypar, D., Gross, M.: Particle-based fluid simulation for interactive applications. *Proceedings of the 2003 ACM SIGGRAPH/Eurographics symposium on Computer animation*, 154–159 (2003)
17. Samaras, A. G., Karambas, T. V., Archetti, R.: Simulation of tsunami generation, propagation and coastal inundation in the Eastern Mediterranean. *Ocean Science* 11(4), 643–655 (2015)
18. Solenthaler, B., Pajarola, R.: Predictive-corrective incompressible SPH. In *ACM transactions on graphics (TOG)* 28(3) 40:1–40:6 (2009)
19. St-Germain, P., Nistor, I., Townsend, R., Shibayama, T.: Smoothed-particle hydrodynamics numerical modeling of structures impacted by tsunami bores. *Journal of Waterway, Port, Coastal and Ocean Engineering* 140(1), 66–81 (2014)
20. Wang, X., Liu, P. L. F.: Numerical simulations of the 2004 Indian Ocean tsunamis-coastal effects. *Journal of Earthquake and Tsunami* 1(03), 273–297 (2007)
21. Yanagisawa, H., Koshimura, S., Goto, K., Miyagi, T., Imamura, F., Ruangrasamee, A., Tanavud, C.: The reduction effects of mangrove forest on a tsunami based on field surveys at Pakarang Cape, Thailand and numerical analysis. *Estuarine, Coastal and Shelf Science* 81(1), 27–37 (2009)